Observation of Multiple Stop Bands in Photonic Bandgap Structures Doped with Organic Dyes**

By *Petr Nozar*,* *Davide DiDomenico*, *Chiara Dionigi*, *Maria Losurdo*, *Michele Muccini*, and *Carlo Taliani*

The dramatic growth of the number of papers dealing with photonic bandgap (PBG) structures indicates the importance of the subject.[1–15]

In this paper we report on the optical properties of self-assembled periodic structures of monodisperse doped polystyrene beads (LATEX).[16–20] Our aim is to study the enhancement of the refractive index contrast using an organic dye (Oil Red EGN) infiltrated into the periodic structure and the influence of the dye absorption on the optical properties of the assembly. We test the validity of the simple analysis of optical spectra in the framework of the Bragg and Snell law. Some considerations regarding dimensions of LATEX suitable for experiments are also drawn.

Similar experiments have been performed by Park et al. on LATEX doped with the organic dye Oil Blue N aggregated as a thin layer (≈12 μm).[20] Measurements of optical spectra reported in the literature[17,20] were performed in transmission configuration; they suffer from some basic disadvantages: Firstly, the wavelengths of the stop band of doped and undoped samples are generally different; secondly, due to the multiple scattering in photonic crystals (PCs) the effective optical thickness of doped and undoped samples are different even if the physical thickness is the same; and thirdly, the absorption in the doped PC is strongly amplified due to multiple scattering, in contrast to the disordered doped sample. Therefore, it seems to be inadequate to use both ordered undoped PCs and disordered doped samples as references for the absorption in the ordered doped PC. Indeed, from our transmission measurements (not reported here) it follows that even at the lowest concentration of dye (1.3×10^{-3} M) used, the absorption of the dye reaches saturation, which manifests itself as an *apparent* bandgap in the transmission spectrum, independent of the incident angle of the light beam.

Therefore, we measured reflectivity spectra of thick samples (≈1.5 mm). As there is zero transmitted intensity, the absorption equals the difference between the intensity of the incoming and reflected beam. Within the gap, the attenuation ratio appears smaller due to absorption, which lowers the reflected intensity of the light (absorption has an opposite effect with respect to the transmission experiments). However, the measured width of the bandgap and its shift with the change of the incident beam angle should not be significantly influenced by absorption.

In the article we use the following terminology: i) The stop band is the energy interval associated with the reflection of light from one "crystallographic" system of planes. ii) If the stop bands of all "crystallographic" systems of the planes have non-zero overlap, the energy interval of this overlap is called a full photonic bandgap. iii) The strong nonlinear behavior of the refractive index as a function of wavelength at the absorption is called the resonance, for convenience.

The synthesis of charged LATEX, their aggregation, doping by an organic dye (Oil Red EGN), and the characterization by atomic force microscopy (AFM) and transmission electron microscopy (TEM) methods is reported elsewhere.[21]

Figures 1a and 1b show typical results of absolute reflectance measurements on undoped LATEX and doped LATEX, respectively. The spectrum of the sample of undoped beads exhibits one main reflectivity maximum, which corresponds to the reflection from the system of (111) planes of the sample. With increasing incident angle γ of the light beam, this maximum is shifted towards lower wavelengths (blue shift), and the intensity of the maximum gradually decreases.

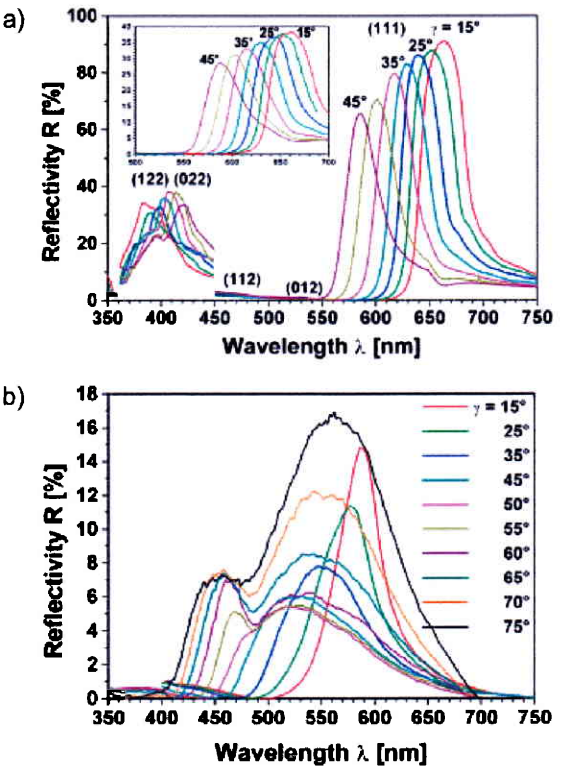

Fig. 1. a) Reflectivity spectra of bare LATEX (D = 295 nm) for different γ ($15° \le \gamma \le 45°$; $\Delta\gamma = 5°$ between two adjacent curves). The numbers in parentheses indicate systems of planes in the position of reflection. Intensities of the spectra in the interval of 360–450 nm are multiplied by 5 for clarity. Reflectivity spectra of the same batch of LATEX doped by dye Oil Red EGN are reported in the inset. b) Reflectivity spectra of a sample of dyed LATEX (D = 245 nm) for different γ.

[*] Dr. P. Nozar, Dr. D. DiDomenico, Dr. C. Dionigi, Dr. M. Muccini, Prof. C. Taliani
Istituto per lo Studio dei Materiali Nanostrutturati, CNR
Via P. Gobetti, 101, I-40129 Bologna (Italy)
E-mail: nozarpetr@libero.it
Dr. M. Losurdo
Plasma Chemistry Research Centre, CNR
Via Orabona, 4, I-70126 Bari (Italy)

[**] Work was supported in part by the European Communities' IST Program under contract IST-2001-33057, ILO and by the European Communities' Human Potential Program under contract HPRN-CT-2000-00135, LAMINATE.

  0935-9648/02/1508-1023 $ 17.50+.50/0

Additional maxima of much lower intensity are observed at lower wavelengths (between 370 and 430 nm for the sample shown in Fig. 1a), in measurements performed on samples with small grains at the surface. These maxima correspond to the reflection from other systems of "crystallographic" planes in the sample ((122), (022), (112), and (012)), because the grains at the surface of the sample show a texture with a surface-parallel "crystallographic" (111) plane, and random orientation in the surface plane. Therefore, all grains contribute to the reflection from the (111) system of the planes. By changing the angle γ, other "crystallographic" systems of different grains fulfil the Bragg condition for reflection. The intensity of additional peaks is much smaller than the (111) reflection because of the small number of grains contributing to these reflections, and because of the lower density of scattering centers (beads) in planes other than the (111) plane. Moreover, the Bragg condition of the other "crystallographic" systems is approached from high reflection angles γ' that gradually decrease, thus increasing the angle γ. Therefore these peaks exhibit a red shift. Spectra measured on samples prepared from the same batch of LATEX and doped with Oil Red are reported in the inset of Figure 1a for comparison. Due to the diameter of the beads, even the stop band of doped PCs is outside of the resonance of the dye. Reflectivity spectra of these samples exhibit a regular variation of the intensity and a blue shift with increasing angle γ—a behavior rather similar to undoped LATEX samples.

Doped PCs, whose stop band falls into the interval of the dye resonance, show a dramatically different behavior (Fig. 1b). With increasing angle γ ($15° \leq \gamma \leq 45°$) the (111) reflection maximum shifts fast to lower wavelengths and the intensity also decreases very fast. Moreover, the maximum broadens significantly. For an incident angle γ in the range of $50° \leq \gamma \leq 75°$ the trend reverses—the position of the maximum starts to shift to longer wavelengths and its intensity increases with increasing angle γ. Additionally, the second peak at shorter wavelengths starts to appear as a shoulder of the main peak and gradually develops into a separate maximum.

As it is mentioned in the literature,[22] the scattering cross section of the individual beads at the Mie resonance[23] is considerably larger than their geometrical cross section. It means that in the densely packed plane (the (111) plane of a face-centered cubic (fcc) structure) the scatterers are optically connected and the plane is optically homogenized. This fact allows us to study the scattering from three-dimensional periodic structures as the Bragg scattering from a one-dimensional stack of planes. However, the limitations of this approximation should be kept in mind in the following discussion.

We will start our discussion by the analysis of the Bragg equation:

$$m\lambda = 2d\, n \cos(\gamma) \tag{1}$$

where m is the order of diffraction, λ is the wavelength in vacuum (and/or air) at which the Bragg condition is fulfilled, d is the separation of the planes in the stack, n is the average refractive index, and γ is the angle between the normal to the scattering plane and the direction of the incoming light beam. The average refractive index of dyed beads is determined by the relation:

$$n = f(k)\, n_{\text{sph}} + z_{\text{eff}}(k,z)\, n_{\text{dye}} + [1-f-z_{\text{eff}}(k,z)]\, n_{\text{air}} \tag{2}$$

where $f(k)$ is the volume fraction of the LATEX, $z_{\text{eff}}(k,z)$ is the effective volume fraction of the dye, n_{sph} is the refractive index of the (non-dyed) LATEX, n_{dye} is the refractive index of the dye, k is the imaginary part of the refractive index of the dye, and $n_{\text{air}} = 1$ in the following discussion. The dye creates a very thin shell on the surface of the LATEX particle, as it has been shown before.[23] The effective volume fraction of the dye $z_{\text{eff}}(k,z)$ is a function of the absorption of the dye and, therefore, the function of the wavelength of the light beam. It could be seen from two limiting cases: a) at wavelengths far from resonance, where the dye absorption is nearly zero, the light is penetrating both the shell created by the dye on the surface of the LATEX bead and the LATEX bead itself. The effective volume fraction $z_{\text{eff}}(k,z)$ is equal to the real volume fraction of the dye in the sample z and there is a contribution from both the refractive index of the dye and the refractive index of the LATEX particle to the average refractive index of the sample. b) At resonance, the absorption of the dye is strong and the high-frequency conductivity $\sigma(\omega)$ is non-zero. The LATEX particle can be screened totally by the shell of the dye (as is the case for a water shell[24]). In such a case the light "sees" only the sphere of dye and $z_{\text{eff}}(k,z)$ corresponds to the sum of the volume fraction f of the LATEX and the volume fraction z of the dye. For this reason we can expect a cut-off of the values of the refractive index n measured on the sample of dyed LATEX for wavelength ranges where the value of the refractive index n_{dye} is still high, but the absorption is already low. Another consequence is an effective dependence of the volume fraction of LATEX particles f on the absorption of the dye—$f(k)$.

In the next part we will consider $m = 1$ and $d = (2/3)^{1/2}D$, where D is the diameter of the bead, as we consider the fcc structure of our samples. The rearrangement of Equation 1 using the Snell law leads to the relation:

$$n(\lambda) = [3\lambda^2/8D^2 + \sin^2(\gamma)]^{1/2} \tag{3}$$

Equation 3 gives us the possibility to find general features for the graphical solution of the Bragg equation. Indeed, both left and right side of Equation 3 are functions of λ and, hence, plotting the functions $f(\lambda) = n(\lambda)$ and $g(\lambda) = [3\lambda^2/8D^2 + \sin^2(\lambda)]^{1/2}$ as independent functions of λ in the same graph with D and λ as parameters gives us the estimate of the overall behavior of our system. The schematic picture of the solutions of the Bragg equation is presented in Figure 2a. It can be seen from Figure 2a that the number of simultaneous solutions (for one set of parameters D and γ) can vary from one to three in the presence of a nonlinear refractive index depending on parameters D and γ. Therefore it should be possi-

  0935-9648/02/1508-1024 $ 17.50+.50/0

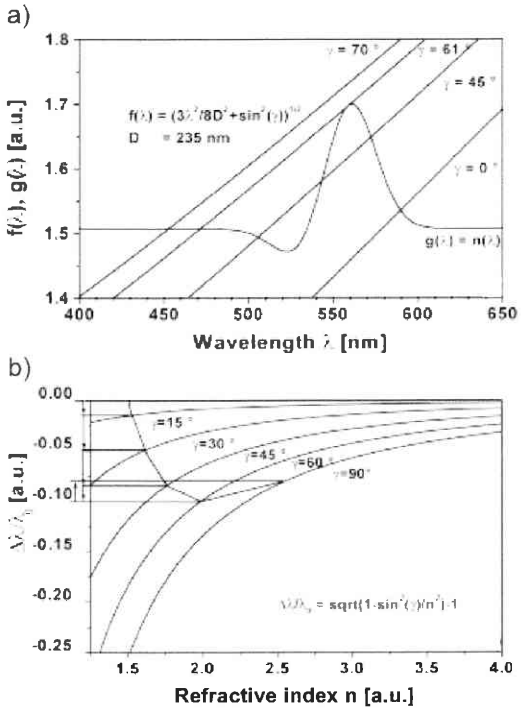

Fig. 2. a) Schematic picture of the solution of the Bragg equation (Eq. 3) Function $g(\lambda)$ represents a hypothetical test refraction index $n(\lambda)$. b) Analysis of the position of the stop band maximum depending on the refractive index n and on the incident beam angle γ (Eq. 4). The full line connecting points on curves for different values of γ represents possible changes of refractive index n changing incident beam angle γ.

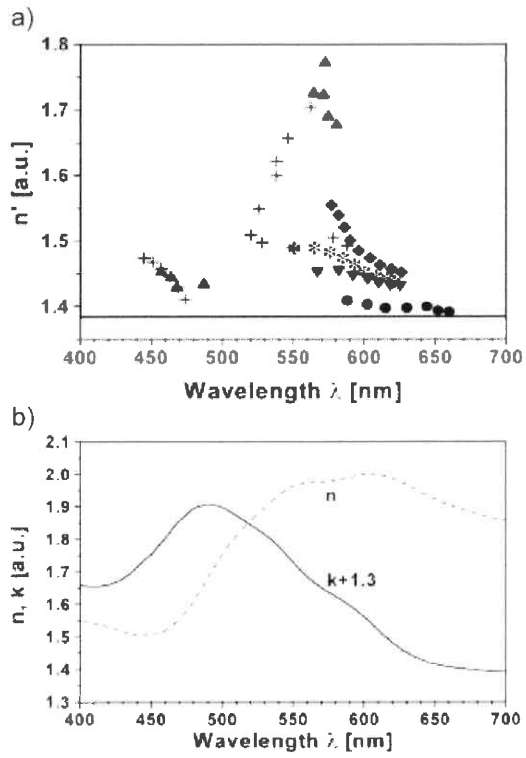

Fig. 3. a) Wavelength dependence of the apparent refractive index n' for different sphere diameters ((solid line) $D=245$ nm bare spheres, (▲) D=200 nm, (+) $D=245$ nm, (*) $D=260$ nm, (▼) $D=265$ nm, (◆) $D=265$ nm (five times higher concentration of the dye Oil Red EGN), (●) $D=95$ nm. b) Wavelength dependence of the real part (n) (dashed line) and imaginary part (k) (solid line) of refractive index of the dye Oil Red EGN. The imaginary part (k) is shifted upwards by 1.3 for clarity.

ble to observe simultaneously up to three stop bands in the spectrum of doped PBG material. Moreover, for a properly chosen diameter D (or a small set of them), it should be possible to "scan" the whole situation. One solution for the long wavelength range (and, thus, low values of γ) could be seen, two and three solutions for the middle wavelength range, and two and one solution(s) for the short wavelengths (highest values of γ) were obtained. However, such scenario is only possible under the condition that the entire wavelength range of solutions of the Bragg equation falls into the range of high absorption of the dye. In other cases there will be a suppression of the part of solutions due to the low value of z_{eff}. Therefore, the refractive index of the doped system, determined from reflectance measurements using Equation 3, is only the apparent refractive index.

Values of the apparent refractive index n' of our samples have been analyzed formally according to Equation 3 as a function of the position of the maximum of the stop band and the incident beam angle γ. The results for different diameters D of the beads and different concentrations of the dye are shown in Figure 3a. Generally, the apparent refractive index n' of the system increases by approaching the absorption edge from the long wavelength region. The peak of the stop band exhibits a relatively large blue shift with increasing angle γ ($15° \le \gamma \le 45°$, Fig. 1b). Simultaneously, $n'(\lambda)$ is almost constant in the range of wavelengths, where we would expect its resonance (Fig. 3a). This behavior is followed by a *red* shift of the maximum of the stop band ($50° \le \gamma \le 75°$, Fig. 1b) connected to the strong increase of n' and of the absorption. Finally, the apparent refractive index n' exhibits low values in the lower wavelength interval and is growing with decreasing λ, as is again expected. The lower wavelength interval is corresponding to the low wavelength solution of the Bragg equation. From the analysis of the relation for the relative shift of the maximum of the stop band

$$\Delta\lambda/\lambda = [1-\sin^2(\gamma)/n^2]^{1/2} \quad (4)$$

follows that, within the approximation of the Bragg law, the displacement of the maximum of the stop band with incident beam angle γ can be non-positive only (Fig. 2b). As the value $\Delta\lambda$ is measured always with respect to the position λ_0 of the maximum of the stop band for an incident light angle $\gamma = 0$, there is a range of small incident angles and low values of n for which the stop band exhibits a blue shift. However, for high incident angles and simultaneously in the vicinity of the maximum of the refractive index the conditions could be fulfilled in such a way that the reflection maximum shows a *red* shift with respect to the preceding values for $\gamma \neq 0$ (Fig. 2b). However, $\Delta\lambda$ remains always non-positive with respect to λ_0.

  0935-9648/02/1508-1025 $ 17.50+.50/0

From comparison of experimental points for different bead diameters (e.g., $D = 200$ and 245 nm, Fig. 3a) follows that the transition from blue shift to red shift of the reflectivity maximum takes place at different incident angles ($\lambda = 35°$ for $D = 201$ nm, $\gamma = 55°$ for $D = 245$ nm). This is in contradiction with Figure 2b as the curves of the graph do not depend on D.

The central peak of the reflectance curve (Fig. 1b) should be composed of two maxima, which correspond to two different solutions of the Bragg equation (Fig. 2a). Instead, we observe only one broad featureless maximum. Actually, examining the wavelength dependence of the real part (n) and imaginary part (k) of the refractive index of the Oil Red EGN (Fig. 3b) it is seen that the long-wavelength solution of the Bragg equation falls into the range of low absorption. Hence, this solution is suppressed due to the low value of z_{eff}.

It seems reasonable that in the wavelength range where the refractive index $n(\lambda)$ exhibits a relatively large value at the resonance the conditions for the assumption of the one-dimensional stack of optically homogeneous planes breaks down. The simple analysis in terms of the Bragg equation as mentioned above is not valid any more in such a case and a complete three-dimensional computational treatment is needed. However, the calculations need to be done in a self-consistent way, because the periodic potential is now dependent on the wavelength of the light used for the measurement through the wavelength-dependent refractive index and the absorption. The width of the reflectivity maximum is another supporting fact for the breakdown of the assumption of optically homogeneous planes. The reflectivity maximum for higher values of γ extends even to *longer* wavelengths than the maximum measured with the incident beam angle $\gamma = 15°$ (Fig. 1b). This behavior cannot be explained in terms of the simple analysis mentioned above. The other interesting experimental fact is the increasing intensity of the maximum with increasing refractive index $n(\gamma)$. Figure 4 shows the intensity data for bare LATEX and for the LATEX dyed by Oil Red EGN. The intensity of the reflection from the sample of bare beads decreases linearly with decreasing $\cos(\gamma)$. The intensity of the reflection from the sample of dyed beads decreases faster than linearly for low values of γ due to the strong increase of absorption. This corresponds to the crossing of the absorption edge of Oil Red EGN by the stop band. However, this trend reverts for higher values of γ, where the stop band is positioned at the center of the absorption band. The intensity increases with increasing γ and reaches values higher than the intensity for $\gamma = 15°$. This could suggest that there is a gradual enhancement of the optical stop band with increasing $n(\lambda)$, even if the present values of $n(\lambda)$ are still far from the values needed for the opening of a full photonic bandgap.[25,26] Even if we can not quantitatively evaluate the absorption in the doped PC at different incident beam angle γ, we have demonstrated experimentally that the absorption of a doped PC, whose stop band falls outside of the dye resonance, behaves similarly to the absorption of an undoped PC (i.e., a monotonic decrease of the maximum intensity with increasing incident beam angle γ up to the highest measured angles 75° is seen—see inset of Fig. 1a). Therefore, the specific behavior of the reflectivity spectra of doped PCs, whose stop band falls in the range of high dye absorption, is due to photonic bandgap effects.

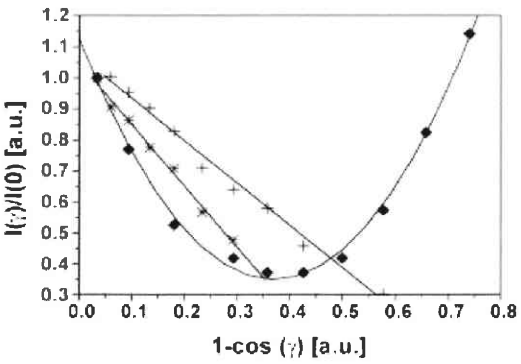

Fig. 4. Comparison of the reflected intensity data for the bare LATEX spheres ((+) $D = 260$ nm, (✳) $D = 245$ nm) and for the LATEX spheres dyed by Oil Red EGN ((◆) $D = 245$ nm). Full lines are guides for the eye.

There are some simple geometrical constraints that need to be considered together with the constraints following from the Bragg equation (Eq. 1 and 3) and the Equation 2 on the value of the refractive index of the doping dye and on the diameter of the beads D. Taking into account the condition of the refractive index ratio $n_{dye}/n_{air} \geq 2$[25] ($n_{dye}/n_{air} \geq 2.8$[26]) for the opening of the photonic bandgap, the refractive index of the dye at the resonance must reach at least the value $n_{res} \sim 2$ ($n_{res} \sim 2.8$). On the other hand, this value together with the value of the wavelength of the resonance maximum of the refractive index of the dye (taken as 565 nm for Oil Red EGN with regards to z_{eff}) determines also the diameter of the beads that can exhibit photonic bandgap behavior. From Equations 1 and 3 follows that $D \leq 173$ nm ($D < 124$ nm) for Oil Red EGN. It is then rather improbable to observe the full photonic bandgap for the fcc assembly of LATEX with a diameter $D \approx 240$ nm dyed by Oil Red EGN.

From the above discussion follows that the infiltration of a periodic structure, which demonstrates an optical stop band, with a suitable organic dye helps to enhance this stop band. From the application point of view this effect is hindered by the strong absorption of the light by the organic dye. In fact, the strongest enhancement of the optical stop band is demonstrated in the wavelength range of the maximum absorption of dye due to z_{eff}.

The analysis of the optical spectra measurements in terms of the Bragg and Snell laws is successful in the wavelength ranges outside of the resonance of the organic dye. In fact, the discussion of the wavelength dependence of z_{eff} is going already beyond this simple picture. In the wavelength range of the resonance of the dye, where a strong enhancement of the optical stop band is observed, the full three-dimensional computational treatment should be used.

Finally, the strong absorption of the light by a system doped by an organic dye requires considerations restrictive with respect to the type of suitable optical measurements. Moreover,

  0935-9648/02/1508-1026 $ 17.50+.50/0

the requirement to reach high enough refractive index values to open a full photonic bandgap puts geometrical constraints on the periodicity of the system with respect to the position of the resonance of the organic dye in the optical spectrum.

Received: October 31, 2001
Final version: April 30, 2002

[1] E. Yablonovitch, *Phys. Rev. Lett.* **1987**, *58*, 2059.
[2] J. E. G. J. Wijnhoven, W. L. Vos, *Science* **1998**, *281*, 802.
[3] O. D. Velev, P. M. Tessier, A. M. Lenhoff, E. W. Kaler, *Nature* **1999**, *401*, 548.
[4] G. Subramanian, K. Constant, R. Biswas, M. M. Sigalas, K. M. Ho, *Appl. Phys. Lett.* **1999**, *74*, 3933.
[5] H. Kajii, Y. Kawagishi, H. Take, K. Yoshino, A. A. Zakhidov, R. H. Baughman, *J. Appl. Phys.* **2000**, *88*, 758.
[6] M. Deutsch, Yu. A. Vlasov, D. J. Norris, *Adv. Mater.* **2000**, *12*, 1176.
[7] S. H. Park, Y. Xia, *Adv. Mater.* **1998**, *10*, 1045.
[8] E. Chomski, G. A. Ozin, *Adv. Mater.* **2000**, *12*, 1071.
[9] O. D. Velev, E. W. Kaler, *Adv. Mater.* **2000**, *12*, 531.
[10] H. Míguez, F. Meseguer, C. López, M. Holgado, G. Andreasen, A. Mifsud, V. Fornés, *Langmuir* **2000**, *16*, 4405.
[11] Yu. A. Vlasov, N. Yao, D. J. Norris, *Adv. Mater.* **1999**, *11*, 165.
[12] Y. Xia, B. Gates, Y. Yin, Y. Lu, *Adv. Mater.* **2000**, *12*, 693.
[13] See *Adv. Mater.* **2001**, *13*, No. 6.
[14] A. Blanco, E. Chomski, S. Grabtchak, M. Ibisate, S. John, S. W. Leonard, C. López, F. Meseguer, H. Miguez, J. P. Mondia, G. A. Ozin, O. Toader, H. M. van Driel, *Nature*, **2000**, *405*, 437.
[15] K.-H. Lin, *Phys. Rev. Lett.* **2000**, *85*, 1770.
[16] K. Yoshino, S. Tatsuhara, Y. Kawagishi, M. Ozaki, A. Zakhidov, Z. V. Vardeny, *Jpn. J. Appl. Phys.* **1998**, *37*, L1187.
[17] Y. Xia, B. Gates, S. H. Park, *J. Lightwave Technol.* **1999**, *17*, 1956.
[18] S. G. Romanov, T. Maka, C. M. Sotomayor-Torres, M. Müller, R. Zentel, *J. Lightwave Technol.* **1999**, *17*, 2121.
[19] S. Gaponenko, V. N. Bogomolov, E. P. Petrov, A. M. Kapitonov, D. A. Yarotsky, I. I. Kalosha, A. A. Eychmüller, A. L. Rogach, J. McGilp, U. Woggon, F. Gindele, *J. Lightwave Technol.* **1999**, *17*, 2128.
[20] S. Park, B. Gates, Y. Xia, *Adv. Mater.* **1999**, *11*, 462.
[21] C. Dionigi, unpublished.
[22] S. G. Romanov, C. M. Sotomayor-Torres, in *Handbook of Nanostructured Materials and Nanotechnology* (Ed: H. S. Nalwa), Academic Press, New York **2000**, Ch. 4.
[23] H. C. van de Hulst, *Light Scattering by Small Particles*, Dover Publications, New York **1981**, Ch. 9.
[24] H. C. van de Hulst, *Light Scattering by Small Particles*, Dover Publications, New York **1981**, Ch. 14.
[25] K. M. Ho, C. T. Chan, C. M. Soukoulis, *Phys. Rev. Lett.* **1990**, *65*, 3152
[26] K. Bush, S. John, *Phys. Rev. E* **1998**, *58*, 3896.

Multi-Colored Photochromic Crystals of Diarylethene Mixtures**

By *Masakazu Morimoto*, *Seiya Kobatake*, and *Masahiro Irie**

Photochromism is referred to as a reversible transformation between two isomers having different absorption spectra by photoirradiation.[1,2] Although a large number of photochromic compounds have been reported, compounds that undergo photochromic reactions in a crystalline phase are very rare. Typical examples of crystalline photochromic compounds are paracyclophanes, triarylimidazole dimers, diphenylmaleronitrile, aziridines, 2-(2′,4′-dinitrobenzyl)pyridine, *N*-salicylideneanilines, and triazines.[3–11] In most cases, the photogenerated isomers are thermally unstable. Recently, we have developed thermally irreversible and fatigue resistant photochromic diarylethene crystals.[12–26] The diarylethene crystals have following characteristic properties: i) thermal stability of both isomers, ii) high photocyclization quantum yields, and iii) rapid response in less than 10 ps. The photochromic crystals can be applied to optoelectronic devices, such as optical memory, optical switching, and displays.[27–30]

Multi-component systems of diarylethenes have been reported for the first time by Lehn et al.[31] They demonstrated that absorption properties of the multi-component mixture in solution as well as on silica-gel plates can be modulated by controlling the wavelength, duration, and slit-width of the irradiation applied. In this study, we prepared single crystals of diarylethene mixtures. If the single crystal contains different kinds of diarylethenes, the crystal is expected to exhibit various colors by photoirradiation. The single crystal prepared in this study contains 1,2-bis(2,5-dimethyl-3-thienyl)perfluorocyclopentene (**1a**) and 1,2-bis(2-methyl-5-*p*-methoxyphenyl-3-thienyl)perfluorocyclopentene (**2a**), of which closed-ring isomers have different absorption spectra (Scheme 1). The colorless crystal turned purple, red, or blue by irradiation with different wavelengths of light.

First, photochromism in solution was examined. Upon UV irradiation, the colorless hexane solutions of **1a** and **2a** turned red and blue, respectively. These color changes are due to the formation of the closed-ring forms **1b** and **2b**. The absorption maxima in the visible region were observed at 505 and 592 nm for **1b** and **2b**, respectively. The red and blue colors disappeared upon irradiation with visible light ($\lambda > 450$ nm) and the absorption spectra returned to those of **1a** and **2a**.

A colorless crystal was obtained by recrystallization of a mixture of **1a** and **2a** (90:10) from ethanol. When the ratio of **2a** in the solution was increased, the quality of crystals became poor. The crystal shape was a rhombus and similar to that of the single crystal of **1a**.[15] Figure 1 shows the shape of the crystal. The crystal consists of six surfaces with four rectangles (surfaces A and A') and two parallelograms (surface B). A part of the crystal was dissolved in hexane to measure the composition ratio of **1a** and **2a** by HPLC. The ratio of **1a** and **2a** in the crystal was 99:1. X-ray crystallographic analysis of the crystal **1a**/**2a** showed that the crystal structure was crystallographically the same as that of the crystal **1a** and the presence of **2a** could not be discerned. **1a** molecules were oriented diagonally across the surface B.[15]

The colorless crystal **1a**/**2a** turned purple upon irradiation with 370 nm light. The absorption spectrum for the surface A is shown in Figure 2a. The absorption band has a maximum at 535 nm and a shoulder around 650 nm. The absorption maximum of 535 nm is the same as that observed for the UV-irradiated single crystal **1a**, which is shown in Figure 2d. By partially bleaching with 692 nm light, the purple crystal turned red. The absorption spectrum is shown in Figure 2b.

[*] Prof. M. Irie, M. Morimoto, Dr. S. Kobatake
Department of Chemistry and Biochemistry
Graduate School of Engineering, Kyushu University
Hakozaki 6-10-1, Higashi-ku, Fukuoka 812-8581 (Japan)
E-mail: irie@cstf.kyushu-u.ac.jp

[**] This work was supported by CREST (Core Research for Evolutional Science and Technology) of Japan Science and Technology Corporation (JST).

  0935-9648/02/1508-1027 $ 17.50+.50/0